

Federated Reinforcement Learning to Optimize Teleoperated Driving Networks

Filippo Bragato, Marco Giordani, Michele Zorzi

Department of Information Engineering, University of Padova, Italy.

Email: {filippo.bragato, marco.giordani, michele.zorzi}@dei.unipd.it

Abstract—Several sixth generation (6G) use cases have tight requirements in terms of reliability and latency, in particular teleoperated driving (TD). To address those requirements, Predictive Quality of Service (PQoS), possibly combined with reinforcement learning (RL), has emerged as a valid approach to dynamically adapt the configuration of the TD application (e.g., the level of compression of automotive data) to the experienced network conditions. In this work, we explore different classes of RL algorithms for PQoS, namely MAB (stateless), SARSA (stateful on-policy), Q-Learning (stateful off-policy), and DSARSA and DDQN (with Neural Network (NN) approximation). We trained the agents in a federated learning (FL) setup to improve the convergence time and fairness, and to promote privacy and security. The goal is to optimize the trade-off between Quality of Service (QoS), measured in terms of the end-to-end latency, and Quality of Experience (QoE), measured in terms of the quality of the resulting compression operation. We show that Q-Learning uses a small number of learnable parameters, and is the best approach to perform PQoS in the TD scenario in terms of average reward, convergence, and computational cost.

Index Terms—Teleoperated driving, Predictive Quality of Service (PQoS), reinforcement learning (RL).

I. INTRODUCTION

Teleoperated driving (TD) is positioned to revolutionize the automotive industry by enabling remote operations of vehicles with unprecedented levels of precision and safety. In particular, TD systems can replace the human control of the vehicle in case of emergency or malfunctions, e.g., during extreme weather conditions or in hostile environments. Compared to a fully autonomous driving system, where the control of the vehicle is implemented via software onboard the vehicle itself, in TD the vehicle sends perceptions of the environment, acquired by videocamera and Light Detection and Ranging (LiDAR) sensors, to a remote host, called teleoperator. The teleoperator, that can be either human or artificial intelligence (AI), receives data from the vehicle, processes it, and sends commands to the vehicle’s actuators for proper control [1].

For TD to perform safely, the communication between the vehicle and the teleoperator must be reliable and fast. For example, according to the 3rd Generation Partnership Project (3GPP) Release-17 specifications, the end-to-end latency should be less than 50 ms [2]. However, the size of a raw LiDAR frame of 82 200 points is around 1 MB [3]; with

a sensor rate of 30 fps, the resulting data rate is around 240 Mbps, which may be challenging to handle for most networks.

To solve this issue, TD data must be “transformed” before transmission. One option is to compress perceptions before transmission, to reduce the message size and so the link overload. However, the compression time is not negligible, especially on LiDAR frames, and depends on the compression algorithm [4]. Moreover, compression may significantly deteriorate the quality of the raw perception, with possible negative implications for the teleoperator’s performance.

In this context, the research community has been working on Predictive Quality of Service (PQoS) as a solution to optimize TD applications [5]. In PQoS, the TD system receives advance notifications about possible Quality of Service (QoS) degradation, and implements dedicated countermeasures to maintain connectivity with the teleoperator. In our previous works [6], [7] we proposed a new PQoS framework, referred to as RAN-AI, that can identify the optimal compression level for LiDAR data at the application to satisfy network requirements. We proved that RAN-AI can optimize the trade-off between QoS (measured as the latency between the vehicle and the teleoperator) and Quality of Experience (QoE) (measured as the quality of the resulting LiDAR data after compression).¹ Specifically, the RAN-AI uses reinforcement learning (RL) and, in particular, Double Deep Q-Network (DDQN), for network prediction and optimization, even though this approach requires to learn a huge number of parameters, and is therefore computationally slow to convergence.

Therefore, in this paper we investigate some other classes of RL algorithms for PQoS. We evaluate the trade-off between stateless and stateful and between on-policy and off-policy algorithms (where off-policy algorithms, unlike on-policy, use different policies for training and data collection), and consider both linear and Neural Network (NN) approximations of the action-value function. Notably, we compare the following algorithms: (i) Multi-Armed Bandit (MAB), (ii) State-Action-Reward-State-Action (SARSA), (iii) Q-Learning, (iv) Deep SARSA (DSARSA), and (v) DDQN. Following the approach in [8], we train the RL agents in a federated learning (FL) setup, which improves the convergence

¹While QoE is formally defined as the degree of delight or annoyance of the user of an application or service, in the telecom community QoE is measured as the quality of the application, as opposed to more conventional QoS metrics that depend on the network, e.g., to measure the effect that some network optimizations produce on the applications. In this paper, we adopt this second definition, and define QoE as the quality of the data after compression.

time and fairness compared to centralized RL, and promotes privacy and security. We show via simulations in ns-3 that stateful off-policy outperforms stateless on-policy algorithms, and NN approximation is not always better than linear approximation. Finally, we prove that Q-Learning is the best approach to jointly optimize QoS and QoE for PQoS in terms of average reward, convergence, and computational cost.

The rest of the paper is organized as follows. In Sec. II we describe our PQoS framework, in Sec. III we present the RL algorithms for PQoS, in Sec. IV we show our simulation results, and finally in Sec. V we draw the conclusions.

II. PQoS FRAMEWORK

Our PQoS framework is based on [6], and is implemented in ns-3 via the dedicated `ns3-ran-ai` module,² first presented in [7]. The framework consists of the following modules.

a) Scenario: The scenario consists of N vehicles, referred to as User Equipments (UEs), that communicate with the teleoperator. The teleoperator is a remote host co-located with a Next Generation Node Base (gNB), so it also acts as the access point to the core network.

b) Channel and mobility: For the sake of realism, the map of the scenario in which the vehicles move and interact is taken from OpenStreetMap (OSM). Then, the mobility of vehicles is modeled with Simulation of Urban MObility (SUMO) [9]. Finally, the wireless channel between the UEs and the gNB is modeled with Geometry Efficient propagation Model for V2V communication (GEMV2) [10]. Eventually, the channel traces are parsed in ns-3 to get the received power, so as to obtain the actual QoS of the link.

c) Networking: Our `ns3-ran-ai` module for PQoS is built upon the `ns3-mmwave` module,³ which is used to simulate the whole 5G NR protocol stack [11]. We consider User Datagram Protocol (UDP) at the transport layer to reduce the protocol overhead and transmit data faster.

d) Application: We consider the transmission of high-quality high-resolution LiDAR frames, produced at a frame rate f , from the UEs to the teleoperator. In this work, LiDAR frames are modeled based on SELMA [3], a new open-source multimodal synthetic dataset for autonomous driving.⁴

LiDAR frames can be compressed before transmission via Draco, a lossy compression algorithm developed by Google. This choice is motivated by several claims. First, unlike other solutions, Draco is lightweight and fast for both compression and decompression [4], and can be executed in real time at UEs with limited computational power and with no dedicated hardware. Second, it implements up to 31 quantization levels and 11 compression levels, for a total of 341 compression configurations, so it gives the agents many opportunities to learn. For example, a more aggressive compression level can reduce the message size, thus improving latency. On the downside, it increases the (de)compression time, and possibly degrades the quality of the resulting frame.

e) RAN-AI: It implements an RL agent to identify the optimal compression configuration (i.e., the action) for the LiDAR data (and thus the corresponding size of the packets to send), to optimize the trade-off between QoS (i.e., the communication delay) and QoE (i.e., the quality of compression). While in our previous works the RL agent was trained according to the DDQN algorithm, an extended version of the classical Q-Learning, in this paper we study and implement some other possible RL solutions, as described in Sec. III.

III. REINFORCEMENT LEARNING CONFIGURATIONS

RL is a branch of machine learning (ML) that focuses on finding an optimal policy π^* for an environment to maximize the cumulative future reward [12]. Specifically, the RL agent works with the assumption that the environment is a Markov Decision Process (MDP). As such, the environment is modeled as a tuple $\mathcal{E} = (\mathcal{S}, \mathcal{A}, \mathcal{P}, \mathcal{R})$, where \mathcal{S} is the set of states, \mathcal{A} is the set of actions, \mathcal{P} is the transition probability matrix, and \mathcal{R} is the reward function. At time t , the RL agent interacts with the environment observing the current state S_t , takes action A_t , and receives from the environment a reward R_t . Then, based on \mathcal{P} , the environment moves to the next state S_{t+1} where the agent will take the next action A_{t+1} .

The goal of the agent is to find the optimal policy π^* that maximizes the expected return. The return G_t is the cumulative future reward from time t , defined as

$$G_t = \sum_{\tau=0}^{\infty} \gamma^\tau R_{t+\tau}, \quad (1)$$

where $\gamma \in (0, 1)$ is the discount factor that represents the importance of the future rewards.

Since in our setup the probability function \mathcal{P} is unknown, we used model-free algorithms to solve the MDP, i.e., the RL agent(s) collect and use data to approximate the action-value function $q_\pi(s, a)$. In other words, the agent(s) do not have prior knowledge of how their actions will affect the state transitions and/or the rewards. Specifically, $q_\pi(s, a)$, $s \in \mathcal{S}$, $a \in \mathcal{A}$, is a function $\mathcal{S} \times \mathcal{A} \rightarrow \mathbb{R}$ that maps every pair (s, a) to the expected reward obtained by taking action a in state s and following policy π . Therefore, the goal of the RL algorithms is to approximate $q_\pi(s, a)$ well enough to derive the optimal policy π^* . Most RL algorithms must explore the environment to learn π^* . To guarantee the exploration of the environment, we use an ε -greedy policy: at each step, the agent chooses a random action in $a \in \mathcal{A}$ with probability $\varepsilon \in [0, 1]$ (exploration), and with probability $1 - \varepsilon$ the action that maximizes the action-value function (exploitation). The value of ε decreases linearly during training.

For PQoS, RL can be a powerful tool to find the optimal compression configuration for LiDAR data, to minimize the communication delay and satisfy quality constraints. Given its ability to adapt to the actual network conditions, an RL agent can outperform an “a priori” choice of the compression configuration. In this work, we compare different RL algorithms, namely MAB (Sec. III-A), SARSA (Sec. III-B), DSARSA (Sec. III-C), and Q-Learning and DDQN (Sec. III-D). Finally,

²Source code: <https://github.com/signetlabdei/ns3-ran-ai>.

³Source code: <https://github.com/nyuwireless-unipd/ns3-mmwave>.

⁴SELMA dataset: <https://scanlab.dei.unipd.it/selma-dataset/>.

the RL algorithms have been trained in an FL setup [13]. Therefore, vehicles periodically share intermediate learning model updates relative to their action-value approximations to a central entity (e.g., co-located at the gNB with the teleoperator), which aggregates the received data into a global model $Q_G(s, a)$, improving on it iteratively. The resulting global model of the action-value function is then returned to the federated agents, that can further train it on their local data. This setup is used to improve the convergence of the RL algorithms, and guarantee fairness inside the network [8].

A. Multi-Armed Bandit (MAB)

MAB is a stateless RL algorithm that approximates the action-value function $q_\pi(s, a)$ as $Q_t^i(a)$, relative to agent $i \in \{1, \dots, N\}$, based solely on action selections and rewards from previous learning steps, and with no explicit knowledge of the underlying state [14]. In our setup, the number of available actions is finite, so $Q_t^i(a)$ can be represented by a lookup table. So, MAB is simple and lightweight.

Update rule. Since the environment is non-stationary, we use the following custom update rule:

$$Q_{t+1}^i(a) = Q_t^i(a) + \lambda (R_t^i - Q_t^i(a)), \quad (2)$$

where λ is the learning rate. Considering an FL setup, learning updates are aggregated into a global model $Q_G(a)$, which is then returned to the local agents for additional training, i.e.,

$$Q_G(a) = \frac{\sum_{i=1}^N \mathcal{N}^i Q_{t+1}^i(a)}{\sum_{i=1}^N \mathcal{N}^i}, \quad \forall a \in \mathcal{A}, \quad (3)$$

where \mathcal{N}^i is the number of learning steps for agent i since the last federated update.

Summary. MAB is simple and lightweight, even though it cannot remember previous states.

B. State–Action–Reward–State–Action (SARSA)

SARSA is a stateful on-policy RL algorithm that evaluates and improves policy π until it converges to the optimal policy π^* . Compared to stateless solutions, stateful algorithms also exploit a representation of the environment (i.e., the state) to approximate the action-value function $q_\pi(s, a)$. The name of SARSA comes from the tuple $\{S, A, R, S', A'\}$: in the current state (S), an action (A) is taken, and the agent gets a reward (R) going to the next state (S'), where it takes the next action (A'). SARSA updates the action-value function for the current state based on either the current best action or another, exploratory, action with some (typically small) probability, so it is an example of on-policy learning. During exploration, the agent may take suboptimal actions, especially in complex environments, thereby yielding suboptimal results. Still, with a proper design of the learning process, SARSA has been proved to converge to the optimal policy [15].

Since the state is continuous and multidimensional, the action-value function $q_\pi(s, a)$ must be approximated as $\hat{Q}(s, a, \mathbf{w})$, where \mathbf{s} (\mathbf{w}) is a vector of states (weights). The weights are updated at each learning step to minimize the error between $\hat{Q}(s, a, \mathbf{w})$ and $q_\pi(s, a)$. SARSA operates with a

linear approximator, which performs an inner product between the state vector (in homogeneous coordinates) and the weights vector related to a specific action, i.e., $\hat{Q}(s, a, \mathbf{w}) = \mathbf{s} \cdot \mathbf{w}_a$. Therefore, SARSA requires a (non-obvious) linear relationship between the state and the action-value function.

Update rule. Let δ_t^i be the difference between the estimate of the action-value function for agent $i \in \{1, \dots, N\}$ at time $t + 1$ and that at time t , i.e.,

$$\delta_t^i = R_t^i - \bar{R}^i + \hat{Q}(s_{t+1}^i, a_{t+1}^i, \mathbf{w}_t^i) - \hat{Q}(s_t^i, a_t^i, \mathbf{w}_t^i), \quad (4)$$

where \bar{R}^i is the average reward collected from the environment. The update rule can be defined as

$$\mathbf{w}_{t+1}^i = \mathbf{w}_t^i + \alpha \delta_t^i \nabla \hat{Q}(s_t^i, a_t^i, \mathbf{w}_t^i), \quad (5)$$

where α is the learning rate, and $\nabla \hat{Q}(s_t, a_t, \mathbf{w}_t) = \mathbf{s}_t$. The FL setup aggregates the weights into a global model \mathbf{w}_G , where

$$\mathbf{w}_G = \frac{\sum_{i=1}^N \mathcal{N}^i \mathbf{w}_{t+1}^i}{\sum_{i=1}^N \mathcal{N}^i}, \quad (6)$$

that is then returned to the agents for additional local training.

Summary. SARSA is lightweight and guarantees convergence, even though it has limited exploration capabilities.

C. DSARSA

DSARSA builds upon SARSA, so it is another example of a stateful on-policy RL algorithm. However, DSARSA considers an NN approximator for $q_\pi(s, a)$, so it can also represent non-linear functions, even though it is computationally more expensive. In particular, DSARSA uses the state vector \mathbf{s} as the input of an NN with $|\mathcal{A}|$ output neurons (where $|\mathcal{A}|$ is the cardinality of the actions space), each of which represents the action-value function of a specific action. The NN has several blocks, each of which consists of a fully connected layer, a ReLU activation function, and a batch normalization layer.

Update rule. The NN uses the Stochastic Gradient Descent (SGD) algorithm to minimize the error in Eq. (4), and the Adam optimizer to facilitate the convergence of the algorithm. The update rule for the FL aggregation is as in Eq. (6).

Summary. DSARSA allows non-linear approximation of $q_\pi(s, a)$, but is computationally expensive.

D. Q-Learning / Double Deep Q-Network (DDQN)

Q-Learning is the stateful off-policy counterpart of SARSA. Compared to an on-policy approach, off-policy algorithms learn and improve a policy π' while exploring using a different policy. Even though there is no guarantee on the actual convergence to π^* , they have been shown to converge faster, in practice, than their on-policy counterparts [16].

The main difference between SARSA and Q-Learning is in the computation of the error in Eq. (4). In SARSA the error is computed using the action performed by the agent at time $t + 1$, while in Q-Learning the error is computed using the action that maximizes the action-value function at time $t + 1$, regardless of what actions are selected from exploration. Therefore, for Q-Learning, the error δ_t^i for agent i at time t is defined as

$$\delta_t^i = R_t^i - \bar{R}^i + \max_{a \in \mathcal{A}} \left(\hat{Q}(s_{t+1}^i, a, \mathbf{w}_t^i) \right) - \hat{Q}(s_t^i, a_t^i, \mathbf{w}_t^i). \quad (7)$$

TABLE I: Compression time and quality using Draco.

c	q	Configuration	Compression time (ms)	mAP
0	8	8-00	5.17	0.257
	9	9-00	5.22	0.580
	10	10-00	5.50	0.686
5	8	8-05	5.34	0.257
	9	9-05	6.97	0.572
	10	10-05	8.52	0.683
10	8	8-10	8.21	0.257
	9	9-10	9.62	0.574
	10	10-10	11.58	0.683

As usual, the action-value function can be approximated by either a linear or an NN approximator. In the latter case, the model is trained according to the DDQN algorithm described in [17], which is an extended version of the classical Q-Learning approach with improved performance.

Update rule. The update rule is the same as in Eq. (5), but with the error defined in Eq. (7). The update rule for the FL aggregation is as in Eq. (6).

Summary. Q-Learning and DDQN have good and fast exploration capabilities, even though convergence is not guaranteed.

IV. PERFORMANCE EVALUATION

In Sec. IV-A we describe our simulation parameters, while in Sec. IV-B we present our experimental results.

A. Simulation Parameters

a) Communication: We consider 5G NR communication at 28 GHz, using numerology 3. The available bandwidth is 50 MHz, and the transmission power is 28 dBm.

b) Application: We consider LiDAR frames generated at $f = 30$ fps. For Draco compression, we consider compression levels $c \in \{0, 5, 10\}$ using $q \in \{8, 9, 10\}$ compression bits. Overall, we have 9 compression configurations, represented by a pair $c - q$. The compression time has been empirically evaluated using the SELMA dataset and an AMD Ryzen Threadripper PRO 3945WX 12-core CPU processor. The quality of the compression is measured in terms of mean average precision (mAP) obtained by the PointPillars object detector [18] on the SELMA dataset after Draco compression. Compression results are reported in Tab. I.

We deploy up to $N = 10$ vehicles. Based on early simulation results, this value is a good compromise to simulate a congested resource-limited scenario, while satisfying the scalability constraints of the ns-3 simulator.

c) Learning: For a fair comparison, we used the same learning setup for all the RL algorithms described in Sec. III. The state of the environment is represented by a multidimensional vector $S \in \mathbb{R}^{18}$, and consists of the following data:

- The average Signal to Interference plus Noise Ratio (SINR), the average number of symbols in the modulation and coding scheme, the average number of subcarriers;
- The average, the minimum, the maximum, and the standard deviation of the RLC, PDCP, and application delays, and the relative Packet Receipt Rate (PRR).

The reward function depends on both QoS and QoE metrics. The QoS is a function of the communication delay d



Fig. 1: Average reward at the end of the training. We set $N = 5$.

between an agent/vehicle and the teleoperator, while the QoE depends on the mAP m_a obtained when using compression configuration a (i.e., the action). Thus, the reward function is

$$R = \begin{cases} m_a & \text{if } d < d_{\text{KPI}}, \\ -d & \text{otherwise,} \end{cases} \quad (8)$$

where d_{KPI} is the latency requirement of the TD application (set to 50 ms in our simulations [2]). Indeed, the RL algorithms iteratively choose the optimal compression configuration to maximize the QoE without violating the QoS requirement.

The RL algorithms have been trained on SELMA for 1000 episodes of 2400 learning steps, with ε starting from 0.1 and decreasing to 0.0001. For the NN approximator, we consider 4 blocks with 64, 128, 64, and 16 neurons respectively.

B. Experimental Results

a) Learning results: We consider $N = 5$ vehicles, and compare the different RL algorithms in terms of the average reward, which measures the actual performance of the system as it represents the trade-off between QoS and QoE. First, in Fig. 1 we plot the reward at the end of the training. We can see that all stateful algorithms outperform stateless MAB. In fact, while MAB makes decisions based solely on the current reward, stateful algorithms maintain an internal state that encodes past experiences, thereby learning patterns, correlations, and dependencies in the environment, and adapting over time. We also observe that off-policy algorithms (Q-learning and DDQN) are slightly better than on-policy algorithms (SARSA and DSARSA) since they can better explore the environment from the beginning of the learning phase, even if there is no theoretical guarantee of convergence.

To confirm this, in Fig. 2 (top) we plot the average reward of the RL algorithms obtained in the first 100 learning steps of the first episode, that is at the beginning of the training. We can see that SARSA and Q-Learning are faster to converge than DSARSA and DDQN. This is because they use a linear approximator for the action-value function, as opposed to a more complex NN, which needs more interactions with the system to start optimizing the network parameters [19]. Interestingly, a MAB solution, despite its simple design, shows similar performance to DSARSA and DDQN at the beginning of the training, and is a valid approach to optimize PQoS if the system has little time to learn (e.g., for real-time operations).

Conversely, Fig. 2 (bottom) shows the evolution of the average reward in the last 30 episodes, that is at the end of the training. As expected, MAB becomes the worst RL

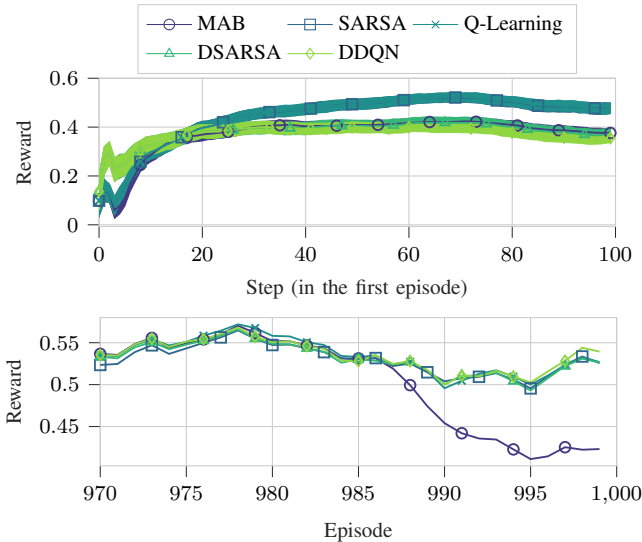


Fig. 2: Average reward over the first 100 steps of the first episode (top) and at the end of the training (bottom), for $N = 5$.

configuration, despite the good training results in the early steps. In fact, as the learning progresses, MAB tends to prioritize exploitation over exploration, and eventually leads to suboptimal outcomes. In turn, stateful algorithms can continuously adapt and learn from previous states, and iteratively adjust their actions to maximize the long-term reward. Notably, even though off-policy algorithms are better than on-policy algorithms, the difference is only marginal. Moreover, the gap between the linear and NN approximation is also marginal. This is because the state is not complex, and the reward function is also linear by design, so a linear approximator can accurately represent the action-value function. Interestingly, DSARSA and DDQN eventually converge to the best solution, though after a longer training process.

In Table II we summarize the performance of the different RL implementations under several metrics, as follows.

- (i) The average reward at the end of the training. As illustrated in Fig. 1, stateful algorithms have similar performance, even though Q-Learning and DDQN eventually outperform the competitors.
- (ii) The average regret, defined as the difference between the current reward and the best possible reward obtained in the same number of steps. This metric determines how quickly the RL algorithms can learn the optimal policy from a random initialization, so it is an indicator of the learning speed. We can see that SARSA and Q-Learning are fast to optimize (the regret is small), while DSARSA

TABLE II: Comparison of the RL algorithms. The best is underlined.

Metric	MAB	SARSA	Q-learning	DSARSA	DDQN
Reward	0.486	0.533	<u>0.535</u>	0.532	<u>0.535</u>
Regret	11.59	<u>3.631</u>	<u>3.631</u>	10.90	9.008
Parameters	9	171	171	19,529	19,529
Operations	0	333	333	37,127	37,127
Time	<u>2.7 μs</u>	0.39 ms	0.52 ms	4.4 ms	5.1 ms

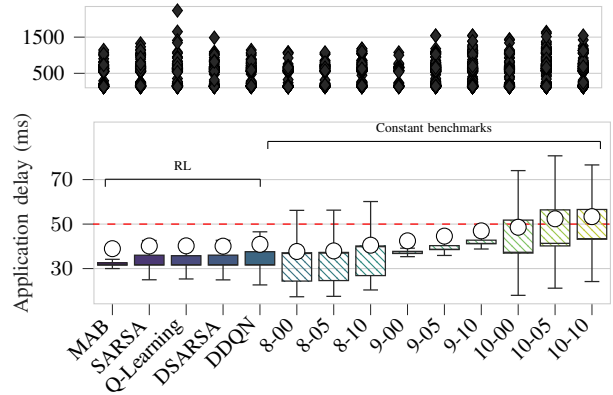


Fig. 3: Average application delay with $N = 10$. Plain (striped) bars are for the RL schemes (constant benchmarks).

- and DDQN are slower because of the underlying NN. The performance of MAB is penalized by the simple setup, and the resulting poor reward as the training progresses.
- (iii) The learnable parameters. DSARSA and DDQN have to learn many training parameters, which justifies the slower convergence, due to the complexity of the NN. In turn, SARSA and Q-Learning only have to learn the vector of weights for each state and action, and the gap with DSARSA and DDQN is at least two orders of magnitude.
 - (iv) The number of arithmetic operations to compute the action-value function in a given state, which is proportional to the computational resources to run the algorithm. For tabular methods like Q-Learning and SARSA, the number of arithmetic operations per update scales linearly with the number of actions, and for MAB it is zero since the action-value function is simply retrieved from a lookup table. For DSARSA and DDQN, instead, the number of operations depends on the complexity of the NN (especially the number of layers and neurons) and on the size of the input space. Notably, DSARSA and DDQN have the same complexity since they use the same NN architecture, and they only differ in the update rule.
 - (v) The (empirical) average time to perform a learning step. We can see that MAB is the fastest, as it almost does not require any computation to update the action-value function. In turn, SARSA and Q-Learning are faster than DSARSA and DDQN, since the latter two require the computation of the NN forward and backward passes.

b) PQoS results: In this paragraph we analyze the performance of RL for PQoS in terms of the application delay (Fig. 3) and the mAP (Fig. 4) for $N = 10$ vehicles. For comparison, we consider constant benchmarks (see Table I) in which the compression configuration is set a priori and does not change during the simulation.

We can see that constant benchmark 8-00 outperforms any other solution in terms of delay since in this configuration data is heavily compressed before transmission, thus reducing the size of the packets to send. However, the resulting mAP is very low. In turn, constant benchmark 10-10 maximizes the

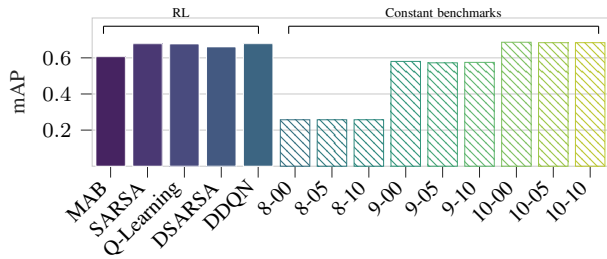


Fig. 4: Average mAP with $N = 10$. Plain (striped) bars are for the RL schemes (constant benchmarks).

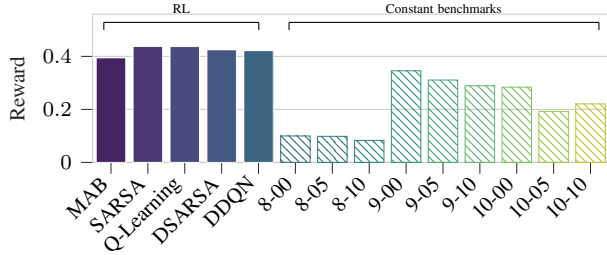


Fig. 5: Average reward after training. Plain (striped) bars are for the RL schemes (constant benchmarks). We set $N = 10$.

mAP as it compresses less, but the resulting delay is almost two times higher than that of 8-00. Notably, RL tries to adapt the compression level to the conditions of the scenario, and achieves the best trade-off between delay (QoS) and mAP (QoE). Most importantly, the application delay is always lower than the TD requirement of 50 ms [2] (represented as a dashed line in Fig. 3), with no degradation in terms of mAP. This is confirmed by the reward in Fig. 5, which is slightly lower than for $N = 5$ (in Fig. 1) since the network is more congested. As expected, every RL scheme, including MAB, outperforms the constant benchmarks, meaning that the adaptive behavior of RL is desirable for PQoS.

Even so, RL comes with several outliers (see the upper part of Fig. 3) where the delay is $\gg 50$ ms, which motivates further research towards more advanced solutions that optimize PQoS relative to every packet transmission, and not only on average.

c) *Design guidelines:* SARSA, Q-learning, DSARSA, and DDQN have a similar reward, while MAB does not converge well. Still, DSARSA and DDQN use an NN approximator for the training, which increases the complexity of the system with limited or no improvements for PQoS. The choice lies between SARSA and Q-learning, with a preference on the latter since it provides the best average reward.

V. CONCLUSIONS AND FUTURE WORK

In this work, we compared different RL algorithms to perform PQoS in a TD scenario. To do so, the agents learn to optimize the compression level of LiDAR data to reduce the transmission delay, without sacrificing the accuracy of the data. We considered different classes of RL algorithms, i.e., MAB, SARSA, Q-Learning, DSARSA, and DDQN, trained in an FL setup to improve convergence and fairness.

We ran simulations in ns-3 to ensure realistic results, and proved that stateful algorithms outperform MAB, and off-policy algorithms with linear approximators are slightly better

than on-policy algorithms. Notably, Q-Learning stands out as a valid, simple, and fast approach to optimize QoS and QoE. Still, it suffers from many outliers in the training, so the performance is optimized only on average.

In the future we will implement a multi-layer PQoS approach to jointly optimize the application and the RAN, and design new RL solutions to minimize outliers in the training.

REFERENCES

- [1] J.-M. Georg, J. Feiler, F. Diermeyer, and M. Lienkamp, "Teleoperated Driving, a Key Technology for Automated Driving? Comparison of Actual Test Drives with a Head Mounted Display and Conventional Monitors," in *21st International Conference on Intelligent Transportation Systems (ITSC)*, 2018, pp. 3403–3408.
- [2] 3GPP, "Service requirements for enhanced V2X scenarios," Technical Specifications (TS) 22.186, 2022.
- [3] P. Testolina, F. Barbato, U. Michieli, M. Giordani, P. Zanuttigh, and M. Zorzi, "SELMA: SEMantic Large-Scale Multimodal Acquisitions in Variable Weather, Daytime and Viewpoints," *IEEE Transactions on Intelligent Transportation Systems*, vol. 24, no. 7, pp. 7012–7024, Jul. 2023.
- [4] F. Nardo, D. Peressoni, P. Testolina, M. Giordani, and A. Zanella, "Point cloud compression for efficient data broadcasting: A performance comparison," in *IEEE Wireless Communications and Networking Conference (WCNC)*, 2022.
- [5] M. Boban, M. Giordani, and M. Zorzi, "Predictive Quality of Service: The Next Frontier for Fully Autonomous Systems," *IEEE Network*, vol. 35, no. 6, pp. 104–110, Nov./Dec. 2021.
- [6] F. Mason, M. Drago, T. Zugno, M. Giordani, M. Boban, and M. Zorzi, "A Reinforcement Learning Framework for PQoS in a Teleoperated Driving Scenario," in *IEEE Wireless Communications and Networking Conference (WCNC)*, 2022.
- [7] M. Drago, T. Zugno, F. Mason, M. Giordani, M. Boban, and M. Zorzi, "Artificial Intelligence in Vehicular Wireless Networks: A Case Study Using Ns-3," in *Proceedings of the Workshop on Ns-3, 2022*.
- [8] F. Bragato, T. Lotta, G. Ventura, M. Drago, F. Mason, M. Giordani, and M. Zorzi, "Towards Decentralized Predictive Quality of Service in Next-Generation Vehicular Networks," *IEEE Information Theory and Applications Workshop (ITA)*, 2023.
- [9] D. Krajzewicz, J. Erdmann, M. Behrisch, and L. Bieker, "Recent development and applications of SUMO - Simulation of Urban MObility," *International Journal On Advances in Systems and Measurements*, vol. 5, no. 3&4, pp. 128–138, Dec. 2012.
- [10] M. Boban, J. Barros, and O. K. Tonguz, "Geometry-Based Vehicle-to-Vehicle Channel Modeling for Large-Scale Simulation," *IEEE Transactions on Vehicular Technology*, vol. 63, no. 9, Nov. 2014.
- [11] M. Mezzavilla, M. Zhang, M. Polese, R. Ford, S. Dutta, S. Rangan, and M. Zorzi, "End-to-End Simulation of 5G mmWave Networks," *IEEE Communications Surveys and Tutorials*, vol. 20, no. 3, pp. 2237–2263, Apr. 2018.
- [12] R. S. Sutton and A. G. Barto, *Reinforcement learning: An introduction*. MIT Press, 2018.
- [13] T. Li, A. K. Sahu, A. Talwalkar, and V. Smith, "Federated Learning: Challenges, Methods, and Future Directions," *IEEE Signal Processing Magazine*, vol. 37, no. 3, pp. 50–60, May 2020.
- [14] V. Kuleshov and D. Precup, "Algorithms for multi-armed bandit problems," *arXiv preprint arXiv:1402.6028*, 2014.
- [15] S. Singh, T. Jaakkola, M. L. Littman, and C. Szepesvári, "Convergence results for single-step on-policy reinforcement-learning algorithms," *Machine learning*, vol. 38, pp. 287–308, Mar. 2000.
- [16] F. S. Melo, "Convergence of Q-learning: A simple proof," *Institute Of Systems and Robotics, Tech. Rep.*, 2001.
- [17] H. van Hasselt, A. Guez, and D. Silver, "Deep Reinforcement Learning with Double Q-Learning," in *Proceedings of the AAAI conference on artificial intelligence*, vol. 30, no. 1, Feb. 2016.
- [18] A. H. Lang, S. Vora, H. Caesar, L. Zhou, J. Yang, and O. Beijbom, "Pointpillars: Fast encoders for object detection from point clouds," in *Proceedings of the IEEE/CVF Conference on Computer Vision and Pattern Recognition*, 2019.

- [19] F. Pase, M. Giordani, G. Cuzzo, S. Cavallero, J. Eichinger, R. Verdone, and M. Zorzi, "Distributed Resource Allocation for URLLC in IIoT Scenarios: A Multi-Armed Bandit Approach," in *IEEE Globecom Workshops (GC Wkshps)*, 2022.